A Study of the Combustion and Emission Characteristics of Compressed-Natural-Gas Direct-Injection Stratified Combustion Using a Rapid-Compression-Machine

S. SHIGA*, S. OZONE, H. T. C. MACHACON, T. KARASAWA, and H. NAKAMURA
Department of Mechanical Engineering, Gunma University, Kiryu, Gunma 376-8515, Japan

T. UEDA and N. JINGU
General Research Center, Nissan Motor Co., Ltd., Yokohama, Japan

Z. HUANG, M. TSUE and M. KONO
Department of Aeronautical and Astronautical Engineering, The University of Tokyo, Tokyo, Japan

The objective of the present study is to determine the characteristics of combustion and emissions of compressed-natural-gas (CNG) direct-injection combustion using a rapid-compression-machine which has a compression ratio of 10 and a disc-shaped combustion chamber. Combustion and emission characteristics are compared for three types of fuel injection (single side, parallel side and opposed side injection) and a homogeneous mixture. The results show that with fuel injection, the fuel could be burned up to an equivalence ratio ϕ of 0.2 with sufficiently high combustion efficiency except for the case of $\phi = 1.0$, while with a homogeneous mixture, the lean burn limit was only $\phi = 0.6$ with poor combustion producing higher unburned CH^4 By adjusting the location of the spark plug and fuel injectors, the combustion limit was extended to $\phi = 0.02$. The Combustion efficiency of the injection modes is over 0.95 except for $\phi = 1.0$ and $\phi < 0.06$ which gave a lower combustion efficiency. Incomplete combustion in the stratified rich zone reduced the combustion efficiency at large values of ϕ, and possible occurrence of bulk quenching resulted in the lower combustion efficiency for very lean mixtures. Combustion efficiency for the homogeneous mixture decreases greatly with leaner mixtures, which is probably due to the thicker quenching layer near the wall. Combustion duration with fuel injection was insensitive to ϕ and was much shorter than for the homogeneous mixture. It was also shown that the number and location of the injectors and the injection rate had little influence on the combustion and the exhaust emissions including NOx. The pressure rise due to combustion in the case of fuel injection is higher compared to that of homogeneous mixture combustion due to the lower heat loss to the combustion chamber walls resulting from a short combustion duration. Thus it is shown that stratified-combustion with extremely lean burn capability can be realized with CNG direct injection.

INTRODUCTION

With the increasing concerns of energy security, much effort has been focused on the development of alternatives for crude oil fuels. One of the promising solutions to this problem is natural gas utilization. While the fuel cell is considered as a future power source, the direct application of natural gas in current internal combustion engines is more realistic. There are also several benefits associated with its use, such as higher thermal efficiency due to the higher octane value and lower exhaust emissions including CO_2 as a result of the small NMOG formation and the lower C/H ratio. For these reasons, natural gas spark-ignition engines have already reached the commercial production stage.

As for the procedure of improving the thermal efficiency of spark-ignition engines, the concept of stratified charge combustion has been realized and is at the same stage of commercial1, 2 production in Japan as the direct-injection gasoline engines [1, 3]. Although stratified charge combustion has an advantage of higher thermal efficiency, the problems of emissions and the limited range of operating conditions need to be addressed. Thus, as with the direct injection gasoline engine combustion, further research on combustion and mixture formation needs to be conducted.

In the present work, the basic characteristics of combustion and emissions of the concept of natural gas fueling combined with stratified charge combustion are studied. Because there is no liquid phase for Compressed-natural-gas

* Corresponding author: E-mail: shiga@me.gunma-u.ac.jp

COMBUSTION AND FLAME 129:1–10 (2002)

Published by Elsevier Science Inc.
0010-2180/02/$–see front matter
PII S0010-2180(01)00367-4

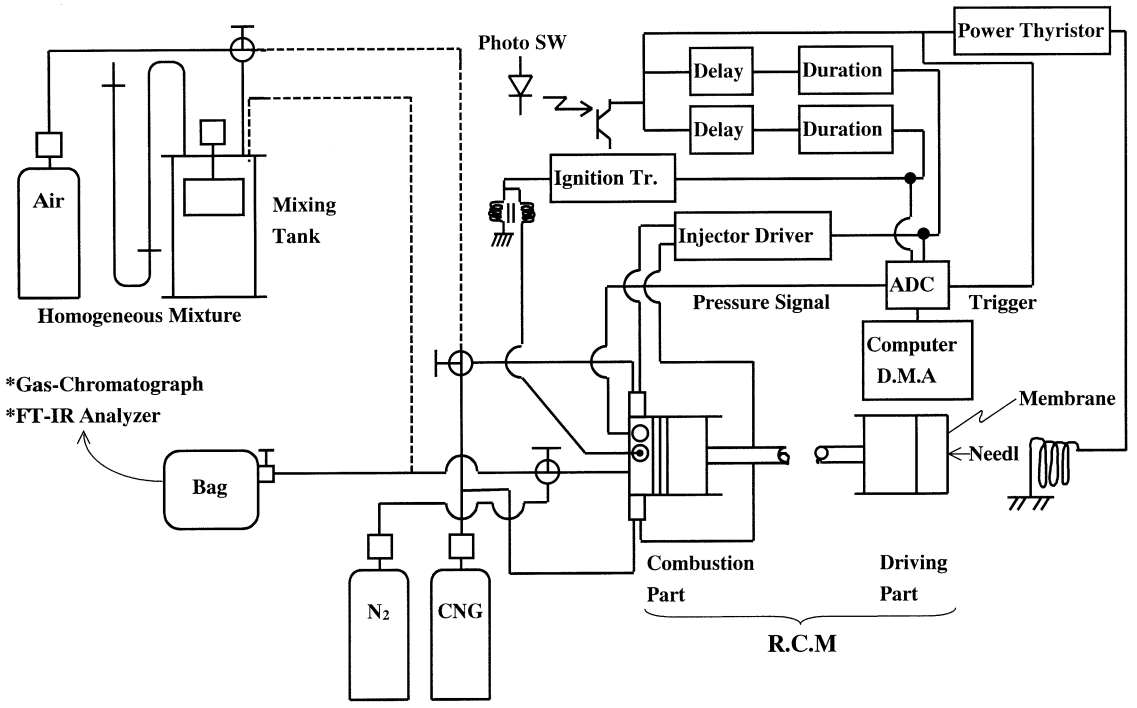

Fig. 1. The experimental setup.

(CNG) direct-injection stratified combustion, no wall wetting exists, and thus, a smaller excessively fuel rich volume can be expected, comparing with the gasoline direct-injection engine. Furthermore, a greater charging efficiency would be achieved than that of a port injection type or gas mixer type CNG engine [4], because the fuel can be injected after closing the intake valve. However, some pressure enhancement device is necessary to inject the fuel into a high-pressure cylinder from the CNG storage when its pressure is lower than the required injection pressure.

The investigation of the concept of CNG direct-injection stratified combustion can be approached in several ways such as engine studies or basic studies of gas jet development and mixing, or combustion bomb experiments. Combustion bomb studies at high pressure and ambient temperature are few, even for gasoline direct injection stratified charged engines which accounts for the serious lack of knowledge needed to solve the problems in actual engines. Very recently, engine studies on the natural gas direct-injection combustion have been published [5, 7]. However, no such studies on 4-stroke spark-ignition (S.I.) engines can be found. As far as the authors' knowledge is concerned, no basic approach has also been found as well as the 4-stroke S.I. engine studies. Thus, a basic approach is necessary in the field of spark-ignition stratified combustion fueled with not only gasoline but also natural gas.

On the basis of this background, the authors opted for a combustion bomb study using a rapid-compression-machine (RCM) to achieve a high pressure and ambient temperature. The cylinder pressure was measured and analyzed, and the exhaust gas components were measured by gas chromatography and by FTIR.

EXPERIMENTAL SETUP AND PROCEDURES

A schematic of the experimental setup is shown in Fig. 1. An RCM was used to achieve a high pressure and ambient temperature [8–10]. Considering the application to S.I. engines, the compression ratio was set at 10. The disc-shaped combustion chamber is 80 mm in diameter and is 20 mm in depth at the end of compression.

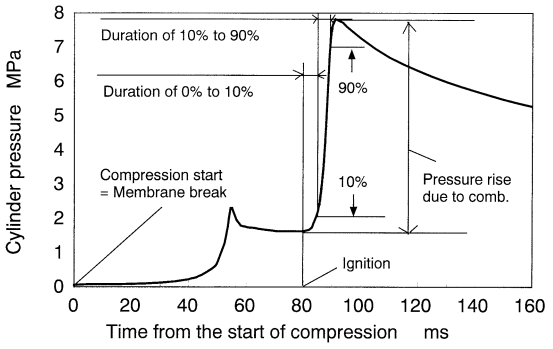

Fijg. 2. Representative cylinder pressure diagram and definitions of the combustion parameters used in this study.

The principle of the machine is the same as that of Kumagai et al. [9], which utilizes the driving mechanism of a shock tube. The start of compression is initiated by the breaking of the membrane separating the driving cylinder and the compressed air reservoir. The breaking signal is taken to be the time reference of this system and the zero of the time scale.

Regarding the reproducibility of this machine, the compression time fluctuates about 10%, but it was revealed that this only results in a 4.3% fluctuation of the compression pressure [8]. Thus, the RCM caused fluctuation can be regarded as low. The injection parameters were measured and calibrated by the manufacturer within the accuracy of the normal engine production level. Considering the high level of accuracy of these hardware systems, the larger scatter of the data at relatively leaner burn conditions is caused by the instability of the ignition and/or combustion phenomenon itself.

Figure 2 shows a representative pressure diagram with several definitions of the parameters for pressure analysis. The main parameters were (1) pressure rise as a result of combustion, (2) initial flame development duration (duration from 0–10% pressure rise as a result of combustion) and (3) main combustion duration (duration from 10%–90% pressure rise as a result of combustion).

Locations of the fuel injectors and the spark gap are shown in Fig. 3. For a centrally positioned spark gap, the two injectors were set at two different locations to see the effect of mutual impingement of the gas jets (which was expected to generate greater mixing between the gas fuel, air and the combustion products) resulted in better utilization of air and so-called internal EGR. The internal EGR might be expected if a part of the burned gas can be recirculated into the unburned region after it is cooled through heat exchange with the surrounding air. The injector locations are labeled as “Opposed Injection” and “Parallel Injection” as shown in (a) and (b), respectively. When the spark gap was set halfway between the center and the side wall (near the injector tip), the fuel was injected through the injector closer to the gap (right hand side of the figure). This is labeled as “Single Injection”.

Dry air was used for the study, and the initial condition for fuel injection was set at the atmospheric condition. To make an accurate comparison between fuel injection and homogeneous mixture combustion, the initial pressure for the homogeneous mixture before compression should be adjusted to a pressure slightly higher than atmospheric pressure p_{atm} according to the equivalence ratio and is given by Eq. 1.

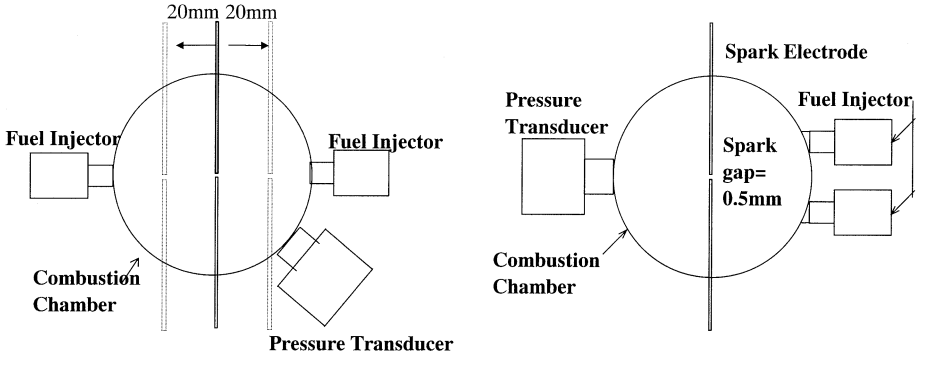

Fig. 3. Arrangements of the fuel injectors and the spark gap. (a) O. Inj. & S. Inj., Spark gap at center & halfway between center and wall. (b) P. Inj., with spark gap at center.

$$p = \frac{0.5\phi + 4.773}{4.773} \cdot p_{atm} \quad (1)$$

This adjustment will maintain the same mass of fuel and air inside the cylinder and create the same condition for combustion. The initial air or mixture (for homogeneous condition) is compressed because of the piston movement caused by the breaking of the membrane which separates the driving cylinder and the compressed air reservoir. Combustion products were analyzed by a gas chromatograph and by an FTIR analyzer (Horiba MEXA4000FT) which can measure 21 species including HC, CO, NO, NO_2, CO_2, and H_2O.

Timings of Fuel Injection and Ignition

In the experiments, the ignition timing was fixed at 80 ms from the start of compression for all conditions and the fuel injection timing was varied to ensure stable ignition and to examine the effect of injection timing. The injection timing for the case of twin injectors was set at 60 ms from the start of compression when the equivalence ratio is greater than or equal to 0.6. The injection timing for the case of a single injector was set at 50 ms from the start of compression when the equivalence ratio is greater than or equal to 0.6. When the equivalence ratio is less than 0.6, the injection timing was adjusted to give the best ignitability for the two kinds of twin injection and the single injection.

Because the injection pressure was kept constant at 9 MPa, which is a far greater value than the choking condition, the mass of fuel injected was determined only by the injection duration.

RESULTS AND DISCUSSIONS

Heat Release Analysis Using a Single Zone Model Based on the Cylinder Pressure

A heat release analysis was carried out using a single zone thermodynamic model based on the cylinder pressure. Because the combustion occurs at a constant volume condition, the energy conservation equation during the combustion process can be simplified as:

$$\frac{dQ_B}{dt} = m \cdot C_v \frac{dT}{dt} + \frac{dQ_w}{dt}, \quad (2)$$

where $\frac{dQ_B}{dt}$ is the rate of heat release, $\frac{dQ_w}{dt}$ is the rate of heat transfer,

$$\frac{dQ_W}{dt} = h_c \cdot A\,[(T - T_W) + 8.5 \times 10^{-11} \cdot (T^4 - T_W^4)], \quad (3)$$

where h_c is the heat transfer coefficient, A is the surface area, T_W is the wall temperature and T is the gas temperature. For many flow geometries, such as flow through a pipe and over a plate, h_c is given by

$$\left(\frac{h_c L}{k}\right) = const. \times \left(\frac{\rho v L}{\mu}\right)^m \left(\frac{c_p \mu}{k}\right)^n \quad (4)$$

where L and v are the characteristic length and velocity, respectively. The terms in brackets from left to right are the Nusselt, Reynolds, and Prandtl numbers, respectively. For gases, the Prandtl number is about 0.7. Annand developed the following correlation on the basis of a concept to match the experimental data to the selected cylinder head location in engines [11].

$$\left(\frac{h_c D}{k}\right) = a \left(\frac{\rho C_m D}{\mu}\right)^b \quad (5)$$

In this equation, the value of a varied with the intensity of charge motion and engine design. For normal combustion, $0.35 \leq a \leq 0.8$ with b constant at 0.7, where the coefficient a tends to increase with increasing intensity of turbulence. k is the thermal conductivity and is given by $k = \mu \cdot C_p/0.7 \cdot Re$ is the Reynold's number which is calculated by $R_e = \rho \cdot D \cdot C_m/\mu$, and μ is the charge viscosity which can be obtained by $\mu = 3.3 \times 10^{-7} T^{0.7}$ kgm^{-1} s^{-1}.

The heat transfer analysis in engines described above is similar to that adopted for a low-speed large engine with disc-shaped combustion chamber, in which the conditions are similar to RCM [12]. It was found that the analysis procedure is useful with some modification of the equation constants.

The authors also found that there was reasonable consistency in the heat transfer rate between the estimated value using Annand's cor-

relation and the experimental results measured by No et al. in their RCM [13]. Miao and Milton also used Annand's correlation in the prediction of heat transfer under RCM conditions [14]. Thus, Annand's procedure developed for engines is considered to be applicable to an RCM by modifying the parameter appropriately.

In this RCM experiment, the average piston speed C_m was used to calculate the Reynolds number. The value of a was determined by fitting the calculated heat transfer rate for the measured pressure history of this RCM. The best fit was obtained when the value of $a = 0.49$.

Thus, the heat transfer coefficient correlation for this RCM may be expressed as

$$h_c = 0.49 \cdot k \cdot R_e^{0.7}/D \tag{6}$$

After introducing the ideal gas state equation,

$$\frac{dQ_B}{dt} = \frac{C_v \cdot V}{R} \cdot \frac{dp}{dt} + \frac{dQ_W}{dt} \tag{7}$$

The fraction of transferred heat to released heat from the ignition event to the time of peak pressure Q^W/Q^B can be determined as follows,

$$\frac{Q_W}{Q_B} = \frac{\int_{t_0}^{t_{max}} \frac{dQ_W}{dt}\, dt}{\int_{t_0}^{t_{max}} \frac{dQ_B}{dt}\, dt} \tag{8}$$

where t_0 is the ignition timing and t_{max} is the timing of peak pressure arrival.

Combustion Efficiency Calculation from the Exhaust Gas Components

Combustion efficiency η_c can be estimated by the formula [11].

$$\eta_c = \frac{H_R(T_A) - H_P(T_A)}{m_f \cdot H_u} \tag{9}$$

where $H_R(T_A) - H_P(T_A) = \sum_{i,reactants} n_i \Delta h_{f,i} - \sum_{i,products} n_i \Delta h_{f,i}$, in which n_i is the number of moles of species i in the reactants or products, and $\Delta h_{f,i}$ is the standard enthalpy of formation of species i at ambient temperature T_A.

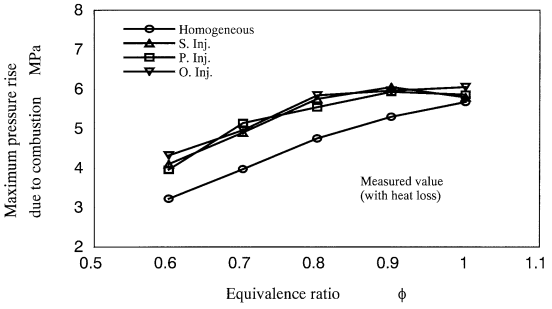

Fig. 4. Maximum pressure rise because of combustion, measured value with heat loss.

In engines, the hydrocarbons and CO measured in the exhaust system by a usual exhaust gas analyzer may be lower than those components remaining at the end of combustion inside the cylinder. This is because of the fact that an appreciable amount of those components would be burned during the expansion and exhaust strokes inside the cylinder and in the exhaust manifold. However, in the present case the mass fraction burned at the end of combustion estimated with the heat release analysis was consistent with the value of combustion efficiency obtained from the combustion products. Therefore, this consistency between the estimated mass fraction burned at the end of combustion and the measured combustion efficiency indicates that there is much less chance of mixing between the unburned mixture remaining at the end of combustion and the burned hot gas in the RCM than in engines. Thus the measured combustion efficiency can be regarded as that at the time of the end of combustion.

Cylinder Pressure

Figures 4 and 5 give the maximum pressure rise due to combustion for different fuel supplying modes in the presence and absence of heat transfer, respectively. The measured maximum pressure rise due to combustion is shown in Fig. 4, and includes the effect of heat loss. There is an obvious difference between fuel injection and homogeneous mixture combustion. The pressure rise because of combustion for fuel injection is higher than that of homogeneous

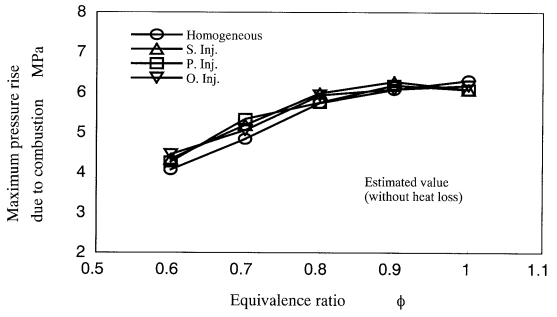

Fig. 5. Maximum pressure rise because of combustion, estimated value without heat loss.

mixture combustion. This indicated that differences in heat loss to the wall of combustion chamber are the main reason for the observed differences in the maximum pressure rise due to combustion. The heat transfer is generally determined by the heat transfer coefficient from the gas to the wall and the duration of the event. For fuel injection, because the mixture is formed in a limited volume and a greater volume close to the wall may have little fuel, the heat transfer coefficient must be lower than that of the homogeneous mixture case. Furthermore, as will be mentioned later, the combustion duration for fuel injection is much shorter than that for homogeneous mixture.

Figure 6 shows the calculated results of the fraction of transferred heat to released heat Q_W/Q_B from the ignition event to the time of peak pressure arrival. It can be seen that the value of Q_W/Q_B for the fuel injection modes is less than that of homogeneous mixture combustion over the whole range of equivalence ratios. This indicates that the heat loss for fuel injection is less than that for homogeneous mixture

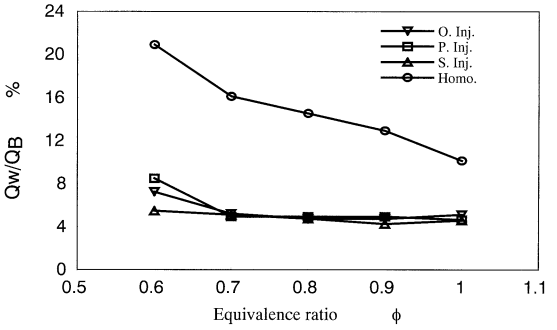

Fig. 6. Ratio of transferred heat to released heat at the timing of peak pressure arrival.

at the time of peak pressure arrival. The estimated maximum pressure rise due to combustion based on the adiabatic combustion process is shown in Fig. 5 and reveals no difference for the different fuel supplying modes. Hence, it is reasonable to conclude that the difference in heat transfer results in the difference in pressure rise observed in combustion using fuel injection and homogeneous mixture.

Effect of Injection Timing

The injection timing was set to three different timings at $\phi = 1.0$ to examine the effect of the injection timing; the earliest, the middle and the latest which were 20, 40, and 60 ms from the compression start, respectively. Because the earliest timing of 20 ms from the compression start is far before the end of compression, little pressure rise can be detected at the time of fuel injection as shown in Fig. 2. At the middle timing of 40 ms from the compression start, an appreciable pressure rise can be seen at the time of fuel injection. The latest timing of 60 ms from the compression start is well after the end of compression. For all three injection timings, the spark timing of 80 ms from the compression start was used as mentioned before. Thus, the fuel injection ends before the spark timing considering that the longest fuel injection duration was 16.7 ms which was for the stoichiometric condition. The injection duration is roughly 2 to 3 times longer than that used in current direct injection gasoline engines. The optimization of the injection duration will be examined together with that of the injection pressure in the next stage of this study.

The pressure rise due to combustion shown in Fig. 7 varies little with the injection timing, while both durations of 0 to 10% (Fig. 8) and 10 to 90% (Fig. 9) pressure rise due to combustion decrease with retarding the injection timing. This result may be caused by two factors; one is the level of mixture stratification and the other is the flow generated by the gas injection. As will be mentioned later, the combustion duration and the heat loss for fuel injection is much less than those for the homogeneous mixture combustion over the whole range of ϕ. This indicates that some stratification still exists at the stoichiometric condition. This stratification be-

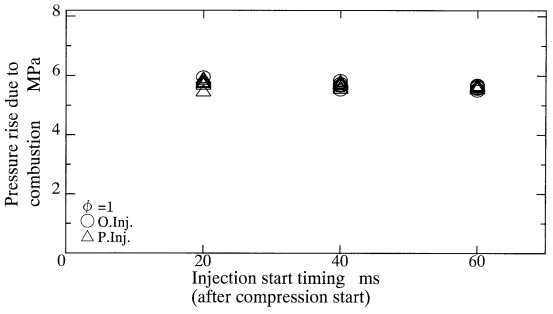

Fig. 7. Variation of maximum pressure rise because of combustion with fuel injection timing.

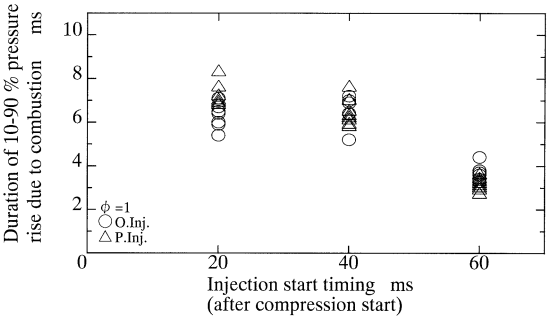

Fig. 9. Variation of main combustion duration with fuel injection timing.

comes weaker with an earlier injection timing. Both durations can be reduced significantly and the average reduction rate of main burn duration of 10 to 90% reaches to almost half. Although this can be expected to reduce heat loss and consequently increase the pressure rise, very little change in the pressure can be seen as described above. This suggests that the reduced heat loss is compensated for by the increased combustion inefficiency due to the excessive stratification, as will be shown later. Thus, the reduction of burning duration does not influence the combustion pressure. Because the injection timing is an important parameter, comprehensive investigation of the effect of injection timing is necessary, and a detailed examination will be reported in the future.

Combustion Pressure and Lean Burn Limit

In Fig. 10, the pressure rise because of combustion is plotted against the equivalence ratio ϕ for homogeneous mixture and three modes of fuel injection. The most prominent difference between the homogeneous mixture and the fuel injection is the limit of combustion. It is only at $\phi = 0.6$ for the case of the homogeneous mixture, and moreover, much unburned CH_4 was detected, which means that the lean burn limit must be practically at $\phi = 0.7$.

In contrast to this, the lean burn limit for fuel injection depends on the injection condition. In the case of 60 ms, which was almost the latest injection timing, the lean limit is almost the same ϕ as that of the homogeneous case. By setting the injection timing at the optimum value which was longer than 60 ms, which means that ignition occurs closer to or during injection, the lean burn limit can be extended to 0.2 which is even leaner than for current direct injection gasoline engine ($\phi = 0.3$) [1–3]. Although comparison with an actual gasoline engine is difficult because of the fact that there are many other parameters in actual engines and that there was no other lean burn enhancement technique applied in this study (such as increasing the turbulence) it is shown that stratified

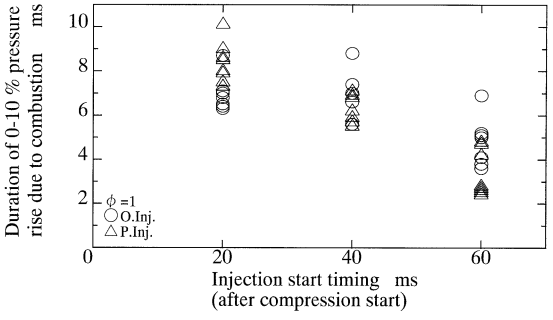

Fig. 8. Variation of initial flame development duration with fuel injection timing.

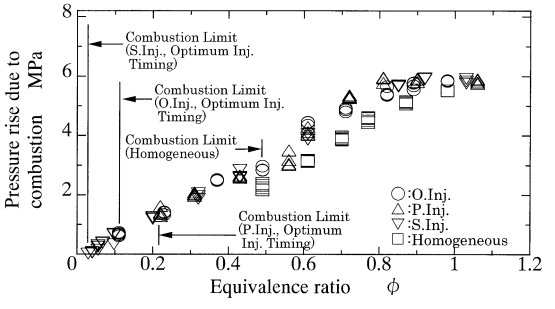

Fig. 10. Maximum pressure rise because of combustion against equivalence ratio ϕ.

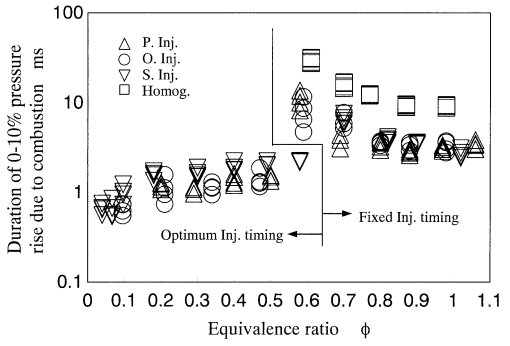

Fig. 11. Initial flame development duration against equivalence ratio ϕ.

combustion with extremely lean burn capability can be realized with CNG direct injection.

By changing the spark gap location from the center position to that closer to the fuel injector and with single injection, the lean burn limit can reach $\phi = 0.02$. This is only 2% of the fuel amount at the stoichiometric condition and is almost the minimum injection rate for the injector hardware used in this study. This encouraging result also indicates the possibility of CNG application to a stratified-charge spark-ignition engine, because it suggests that even at idling conditions, stratified-charge combustion can be applied.

Combustion Duration

The variation of the initial flame development duration and the main combustion duration with ϕ are shown in Fig. 11 and 12, respectively. These are semi-log plots because of the tremendous variation of these combustion durations.

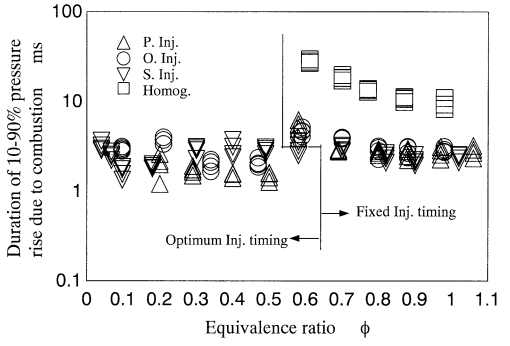

Fig. 12. Main combustion duration against equivalence ratio ϕ.

For the homogeneous mixture, the combustion duration increases as the mixture becomes leaner. In contrast to this, for fuel injection both durations can be classified into two; one is for $\phi \geq 0.6$ and the other is for $\phi \leq 0.5$. In the range of $\phi \geq 0.6$, the dependence of both burn durations (the initial flame development is more remarkable) is similar to that of homogeneous mixture combustion. In the range of $\phi \leq 0.5$, the initial flame development duration decreases with a decrease in ϕ, and the main burn duration roughly takes on a constant value. Considering the fact that in larger regions of ϕ the injection timing was rather early and it was adjusted to the optimum value in smaller regions of ϕ, this may suggest that the combustion pattern for earlier injection is more similar to that of homogeneous mixture combustion. Furthermore, the dependence of burn durations in smaller regions of ϕ is characteristic of stratified combustion. Because these injection timing effects are quite characteristic of the CNG direct-injection combustion, it will be examined in detail and will be reported in the future.

In any event, this behavior must be as a result of the extent of mixture stratification inside the cylinder. This extremely short combustion duration would have contributed to the slightly higher combustion pressure for fuel injection as mentioned earlier.

Furthermore, it is characteristic that the combustion duration for single injection is more or less the same as the other fuel injection conditions. Because the injection rate for each injector is equal within the production accuracy, the injection duration for single injection had to be twice as long as that of parallel injection and opposed injection. Still, results of burn duration and also the combustion pressure in Fig. 10 show the beneficial trend of single injection. This could also be related to the higher level of mixture stratification than the other two types of twin injection, but further research to verify this is needed.

Analysis of Burned Gas Components

Because CH_4 is the major hydrocarbon component in combustion products detected by the FTIR (heated sampling) analyzer, its concentration reflects the state of unburned hydrocarbons

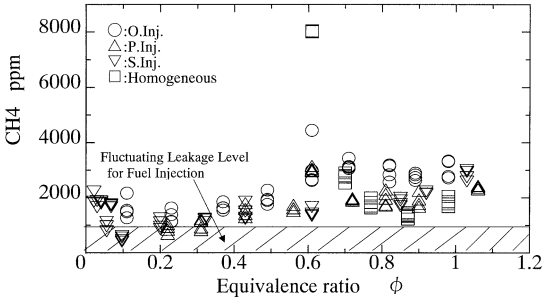

Fig. 13. CH_4 concentration against equivalence ratio ϕ.

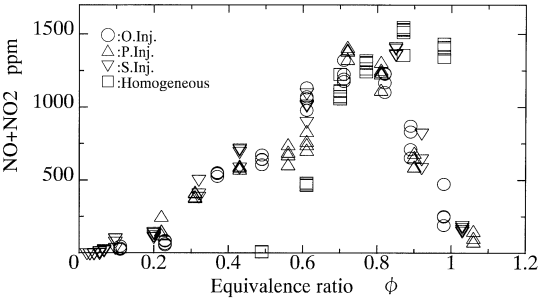

Fig. 15. Variation of NO + NO_2 with equivalence ratio ϕ.

in the combustion products (shown in Fig. 13). For the homogeneous mixture, the CH_4 emission tends to increase with decreasing ϕ. This is a typical trend for the homogeneous lean burn. The unburned hydrocarbons must come from the quenching layer near the wall.

As for fuel injection, it should be noted here that the leakage from the fuel injector was difficult to eliminate and its level varied from trial to trial as shown in the figure. Considering this, all the data points are within the range of measurement of the facility. This suggests that bulk quenching for the stratified charge combustion might be less serious than wall quenching for the homogeneous mixture case.

The calculated combustion efficiency for four different fuel-supplying modes is shown in Fig. 14 [11]. It can be seen that the combustion efficiency of injection modes is over 0.95 except for $\phi = 1.0$ and less than 0.06. At $\phi = 1.0$ because of the stratified mixture formed in the combustion chamber, rich zones exist and combustion efficiency becomes slightly lower. At $\phi \leq 0.06$, the combustion efficiency decreases steeply with decreasing ϕ. This may suggest the possibility of bulk quenching in this extremely low region of ϕ. However, there is a possibility that the leakage from the injector affected the value of the combustion efficiency. We may need to improve the experimental technique and/or facility to examine the phenomenon in such a very lean region.

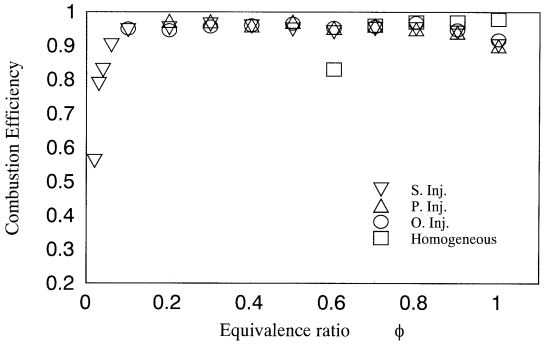

Fig. 14. Variation of combustion efficiency with equivalence ratio ϕ.

NO + NO_2 emission is shown in Fig. 15. For the homogeneous case, the dependence on ϕ is reasonable and the level is low at $\phi = 0.6$. On the other hand, for the fuel injection, the level is high in the region near $\phi = 0.7$, which is characteristic of stratified combustion. For $\phi >$ 0.8, the level decreases steeply. Moreover, the mode of fuel injection did not result in much difference, although it would have been higher than that for single injection if the mixing between fuel and air could be enhanced, and it would have been lower if the internal EGR effect could be realized. As for the injection duration, it has almost no effect on the NOx emission, since there is no difference of NO + NO_2 between single injection and the other injection methods. This is reasonable considering the fact that the combustion duration was little affected by the injection duration as seen in Fig. 6. From close observation, the NO + NO_2 for the single injection is slightly higher than the other twin injection cases at the range of 0.4 to 1.0 of ϕ. This suggests that the extent of stratification for the single injection would be higher than the two other twin-injector cases, which corresponds to the behavior of combustion duration discussed in the previous section. From these results, a general aspect of CNG direct-injection combustion, that the injection parameters seem to have less influence on the

combustion for gas injection stratified combustion, is revealed.

CONCLUSIONS

1. The lean combustion limit for CNG direct injection depends on the timings of injection and ignition. By applying these optimum conditions, it can reach $\phi = 0.02$, with an extremely short combustion duration. This value is much lower than the homogeneous mixture case ($\phi = 0.6$) and the gasoline direct injection engine ($\phi = 0.3$). Thus, stratified combustion with extremely lean burn capability can be realized with CNG direct-injection.
2. The combustion and emission parameters are not significantly influenced by the modes of fuel injection such as the number of injectors, position of the injectors, and the arrangement of the injectors with regard to the spark location. Thus, a general aspect of CNG direct-injection combustion, that the injection parameters seem to have less influence on the combustion for gas injection stratified combustion, is revealed. However, it also appears that single-injection gives higher level of mixture stratification than the twin injection modes.
3. The pressure rise because of combustion for fuel injection is higher compared with that of homogeneous mixture combustion. The difference in heat loss to the combustion chamber wall is regarded as the main reason for the difference, and this was verified by the combustion analysis using a single zone combustion model.
4. Combustion efficiency of fuel injection modes is over 0.95 except for $\phi = 1.0$ and for $\phi < 0.06$. At $\phi = 1.0$, incomplete combustion in the excessively stratified rich zone reduces the combustion efficiency, and at less than $\phi = 0.06$ bulk quenching and/or unavoidable leakage through the injector might have occurred. Combustion efficiency for the homogeneous mixture decreases greatly when the equivalence ratio is 0.6, which is because of a thicker wall quenching in lean homogeneous combustion.

This study was supported by Nissan Motor Co. Ltd., and carried out under the cooperative research program. The authors also acknowledge Shin-nosuke Ishiguro, a student of Gunma University, and Dr. Pin Cai, a research associate of Saitama University for their help with the experiment and the preparation of the manuscript.

REFERENCES

1. Kume, T., Iwamoto, Y., Iida, K., Akishino, K., and Ando, H., SAE Paper, No. 960600 (1996).
2. Iwamoto, Y., Nowa, K., and Nakayama, O., Yamaguchi, T., and Ando, H., SAE Paper, No. 970541 (1997).
3. Matsushita, S., *Proceedings of JSAE Symposium No. 9703,* 33, (1997), (in Japanese).
4. Machacon, H. T. C., Yamagata, T., Sekita, H., Uchiyama, K., Shiga, S., Karasawa, T., and Nakamura, H., *JSAE Review* 21, (4):568. (2000)
5. Hatakeyama, S., Murayama, T., Sekiya, Y., Nakai, S., Sako, T., and Tsunemoto, H., *Proc. of the 16th International Combustion Engine Symposium,* Tokyo, (2000–9), 277, (in Japanese).
6. Shimonagata, T., Kusaka, J., Daisho, Y., Ito, S., Okumura, K., Kihara, R., and Saito, T., ibid, 283.
7. Ishiyama, T., Shioji, M., Kaneko, M., and Okumura, K., ibid, 289.
8. Takahashi, H., Shiga, S., Karasawa, T., and Kurabayashi, T., *JSME Trans., 56* (524) 1218 (1990) (in Japanese).
9. Kono, M., Shiga, S., Kumagai, S., and Iinuma, K., *Combust. Flame* 54(1–3):33 (1983).
10. Takahashi, H., Yanagisawa, H., Shiga, S., Karasawa, T., and Nakamura, H., *Atomizat. Sprays*, 7(1–2):33 (1997),
11. Heywood, J. B., *Internal Combustion Engine Fundamentals*, McGraw-Hill Book Company, New York, 1988, pp. 81 and 678.
12. Taylor, C. F., *The Internal Combustion Engine in Theory and Practice*, The MIT Press, 1985, pp. 273, 277.
13. No, S. H., Kobori, S., and Kamimoto, T. *JSME Trans., 57 (540)*:2833 (1990)
14. Miao, H., and Milton, B. E., *Proceedings of International Symposium on Advances in Computational Heat Transfer*, Sydney, (2000).

Received 24 May 2000; revised 22 October 2001; accepted 1 December 2001